

Distribution Agreement

In presenting this thesis as a partial fulfillment of the requirements for a degree from Emory University, I hereby grant to Emory University and its agents the non-exclusive license to archive, make accessible, and display my thesis in whole or in part in all forms of media, now or hereafter now, including display on the World Wide Web. I understand that I may select some access restrictions as part of the online submission of this thesis. I retain all ownership rights to the copyright of the thesis. I also retain the right to use in future works (such as articles or books) all or part of this thesis.

Brian Kim

April 10, 2024

Collateral Projections of Corticostriatal Neurons in Primates: A Main Source of Inputs to the
Pontine Nuclei and High-Order Thalamic Nuclei

By

Brian Kim

Yoland Smith, PhD

Adviser

Neuroscience and Behavioral Biology

Yoland Smith, PhD

Adviser

Adriana Galvan, PhD

Committee Member

Dieter Jaeger, PhD

Committee Member

2024

Collateral Projections of Corticostriatal Neurons in Primates: A Main Source of Inputs to the
Pontine Nuclei and High-Order Thalamic Nuclei

By

Brian Kim

Yoland Smith, PhD
Adviser

An abstract of
a thesis submitted to the Faculty of Emory College of Arts and Sciences
of Emory University in partial fulfillment
of the requirements of the degree of
Bachelor of Sciences with Honors

Neuroscience and Behavioral Biology

2024

Abstract

Collateral Projections of Corticostriatal Neurons in Primates: A Main Source of Inputs to the Pontine Nuclei and High-Order Thalamic Nuclei

By Brian Kim

Despite significant advances in our understanding of the motor connectome in rodent, our knowledge of the neuropathological changes that affect the morphology and connections of cortical projection neurons in non-human primates remains rudimentary. Extratelencephalic tract (ET) neurons, a type of cortical neuron from layer 5b of the motor cortex, send collateral projections to a number of motor areas in the brain. The lack of efficient tools to characterize the projection targets of specific populations of ET neurons in primates has significantly hampered progress in this area. Current research is limited by single-cell filling and lack of retrograde labeling of axon collaterals which has led to conflicting results on the projection of ET neurons to different brain regions. The recent development of a designer vector variant of recombinant adeno-associated virus serotype 2 (AAV2-retro), with highly potent and selective retrograde transduction properties, addresses some of these limitations. Our findings demonstrate that AAV2-retro is a highly reliable tool to retrogradely label corticostriatal neurons in rhesus monkeys. A major feature that distinguishes this technique, from other retrograde tracing methods, is the prominent labeling of axon collaterals that originate from labeled neurons allowing for the analysis of the connectome of these cells.

Our preliminary data suggests that corticostriatal neurons that project to the putamen give rise to axon collaterals that terminate in the pontine nuclei in rhesus monkeys. After AAV2-retro injections in the putamen, profuse retrograde labeling was found in motor cortices and clusters of labeled axon terminals were seen in the pontine and pulvinar nuclei. Preliminary electron microscopy data from two monkeys showed that these axon terminals form asymmetric (putatively, excitatory glutamatergic) synapses with dendritic or vesicle-filled profiles, suggesting their cortical origin. Double immunolabeling of one of the monkeys indicates labeled terminals are positive for vGluT-1 which further confirms the cortical origin. These results suggest cortical neurons send efference copies of motor commands to the striatum, pons, and thalamus. Further work will determine how this connection is altered in a nonhuman primate model of Parkinson's disease.

Collateral Projections of Corticostriatal Neurons in Primates: A Main Source of Inputs to the
Pontine Nuclei and High-Order Thalamic Nuclei

By

Brian Kim

Yoland Smith, PhD
Adviser

A thesis submitted to the Faculty of Emory College of Arts and Sciences
of Emory University in partial fulfillment
of the requirements of the degree of
Bachelor of Sciences with Honors

Neuroscience and Behavioral Biology

2024

Acknowledgements

I would like to thank Jean-Francois Paré and Susan Jenkins for their technical assistance and training me in the many protocols used for successful preparation of tissue for microscopy. I would also like to thank everyone in the lab that helped me make this project a reality and all of the committee members for giving their expert input on my thesis. I would like to give special recognition to my adviser, Dr. Yoland Smith, who has been extremely supportive since I joined the lab. This work was supported by the ASAP Collaborative Research Network and the NIH based grant of the Emory National Primate Research Center.

Table of Contents

Introduction.....	1
Axon Collateralization.....	1
The Motor Connectome and Species Differences.....	1
Corticostriatal Neurons.....	4
Study Goals.....	6
Methods.....	8
Viral Vector-Mediated Labeling of Cortical Neurons.....	8
Animals.....	8
Immunohistochemistry.....	9
Light Microscopy.....	9
Electron Microscopy.....	10
Immunogold for Electron Microscopy.....	11
Image Analysis.....	12
Light Microscopy.....	12
Electron Microscopy.....	12
Statistical Analysis.....	13
Results.....	14
Localization of Viral Vector Labeling by Light Microscopy.....	14
Ultrastructure Characterization of Corticopontine and Corticothalamic Projections–Electron Microscopy.....	17
Ultrastructure Characterization of Corticopontine Terminals labeled by M1 Anterograde AAV Injection vs Putamen Retrograde AAV Injection.....	22

Discussion.....	24
Collaterals of Corticostriatal Axonal Projections Throughout the Brain.....	24
Immunoreactivity for vGluT1 in Corticostriatal Projection Terminals in Pontine Nuclei and Verification of Morphology in Comparison to Corticopontine and Corticothalamic Neurons.....	25
Differences in Morphology of Postsynaptic Targets Between Collaterals of Corticostriatal Projections in Pontine and Pulvinar Nuclei.....	26
Comparison of Morphology Between Corticostriatal, Corticopontine, and Corticothalamic Terminals.....	27
Limitations for Current Study and Future Directions.....	28
References.....	30

Introduction

Axon Collateralization

Neurons are the basic building block of the brain and the interactions between them process and integrate information to dictate responses made by the organism. A key feature of neurons is the ability to both receive inputs and send outputs to other neurons. The axon of the neuron is a long cord that carries the action potential which causes the release of neurotransmitters at the terminal of the neuron. However, through a phenomenon known as collateralization, the axon can split into a myriad of branches and send outputs to multiple targets (Rockland, 2018). Axon collaterals are a unique anatomical feature that allow neurons to relay a signal to multiple brain regions and keep brain activity in sync. The receiving brain regions can modulate the signal in different ways which makes brain activity and its connections an extremely complex mechanism. Furthermore, all neurons are not made to be the same; there are a diverse number of neuron classes depending on the specific functions required by the brain. In many neurodegenerative diseases, the function and/or connection of these neurons are compromised (Shepherd, 2013). Thus, a comprehensive understanding of the normal and diseased-state connectome can be key in diagnosis, detection, and intervention for those diseases.

The Motor Connectome and Species Differences

The cerebral cortex is comprised of four broad lobes: frontal, parietal, occipital, and temporal (Jawabri & Sharma, 2023). Although each of these lobes are responsible for a variety of different functions, one thing these cortical areas have in common is the innervation of different subcortical regions throughout the brain. The cerebral cortex is composed of six layers parallel to the surface of the brain that differ in laminar size depending on the neocortical region

(Saber et al., 2023). In the primary motor cortex (M1), layer 5 is relatively thicker to other neocortex areas and contains glutamatergic projection neurons vital to movement control that innervate a number of brain regions, including the basal ganglia (BG), thalamus, and brain stem. Specifically, given the role of the BG in movement control, the striatum receives heavy input in its sensorimotor region (post-commissural putamen) from cortical neurons (Shepherd, 2013). Among layer 5 projection neurons, two striatal projecting subclasses of neurons exist: intratelencephalic tract neurons (IT) and extratelencephalic neurons (ET). Generally, IT neurons project bilaterally within the telencephalon (which include the striatum and the cortex itself) while ET neurons project ipsilaterally to a variety of brain regions, both within and outside of the telencephalon, and contralaterally to the brainstem and spinal cord (Reiner et al., 2010; Garcia et al., 2021; Shepherd, 2013). Although both types of neurons have cell bodies in layer 5, ET neurons are exclusively found in layer 5b of the M1 while IT neurons can be found in layers 2 through 6 (Shepherd, 2013). ET and IT neurons give rise to the corticostriatal connections that terminate in the post-commissural putamen.

Non-human primate (NHP) models have been utilized to extensively study cortical projections. ET neuron axon collaterals in NHPs tend to terminate on ipsilateral motor nuclei, such as those of the basal ganglia and motor thalamic areas, which are predicted to assist, among other movements, with dexterity and detailed motor movements of the hand (Jankowska et al., 1975; Bortoff & Strick, 1993; Sinopoulou et al., 2022). Contrary to NHPs, rodent ET neurons are highly collateralized with M1 projections ending in both motor and sensory subcortical brain areas. In a single-cell filling study, individual ET neurons in the M1 of rodents were injected with an anterograde tracer (Kita & Kita, 2012). The study found that single ET neurons project to a number of areas, including the striatum, thalamus, subthalamic nucleus, brainstem, and spinal

cord. A second, more recent rodent study in which the authors constructed the entire corticospinal projectome from retrograde virus injections in portions of the spinal cord responsible for forelimb control in rats (Sinopoulou et al., 2022), axon collaterals of corticospinal neurons were found to terminate in over a dozen regions and were heavily weighted towards sensory and sensorimotor areas (Fig. 1).

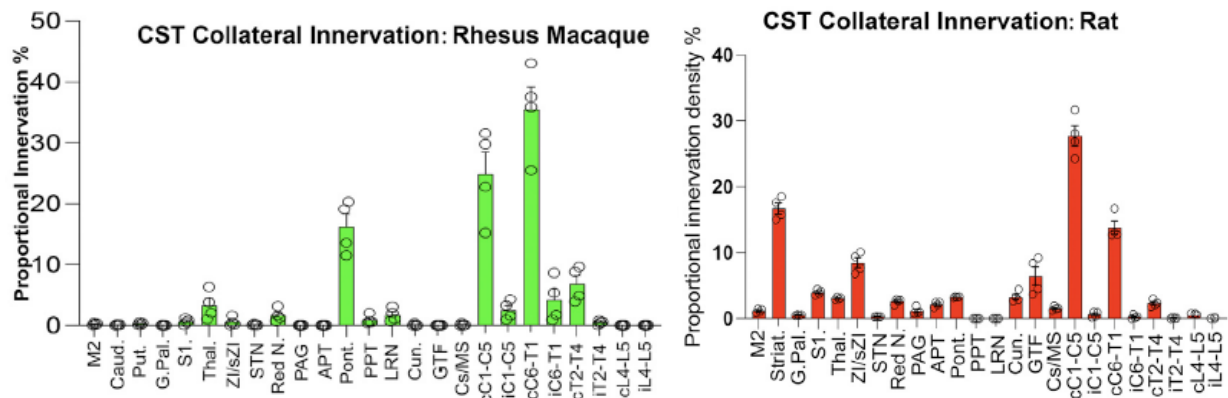


Figure 1. Distribution of corticospinal projections after injection of AAV-rg-retro or AAV9-retro, respectively, in the spinal cord of primates (left) and rodents (right). Abbreviations: M2, sensorimotor cortex; Caud, caudate; Put, putamen; G. Pal, globus pallidus; Striat, striatum; Thal, thalamus; ZI/SZI, zona incerta/subIncerta; STN, subthalamic N.; PAG, periaqueductal gray; APT, anterior pretectal N.; Pont, pontine N.; PPT, pedunculo pontine tegmental N.; LRN, lateral reticular N.; Cun, cuneatus N.; GTF, gigantocellular tegmental field; Cs/MS, superior colliculus/mesencephalic nucleus; C, contralateral; I, ipsilateral. Adapted from “Rhesus macaque versus rat divergence in the corticospinal projectome,” by Sinopoulou et al., 2022, *Neuron*, 110(18), p. 2970–2983. Copyright 2022 by Elsevier.

Based on current literature, there is species-dependent differentiation in ET neuron projections. In the same study, Sinopoulou et al. (2022) describes clear differences in the pattern of axon collateralization between rodent and NHP corticospinal neuron projections (Fig. 1). In comparison to rodents, NHP corticospinal axons are shown to have much more narrow collateral projection systems aimed specifically at subcortical motor areas. Omitting the corticospinal neuron terminals in the spinal cord, there is a proportionately heavy density of projections to the thalamus and pontine nuclei.

However, projectome studies using NHPs are far and few between. There are gaps in knowledge and a lack of understanding of the extent of cortical neuron projections in NHPs especially compared to rodent research. One of the objectives of this project is to shed light on the organization of the connectome of ET corticostriatal neurons in NHPs as the groundwork for improved understanding of the NHP cortical connectome.

Corticostriatal Neurons

The striatum is the predominant structure of the basal ganglia that plays an important role in motor function, motivation, and decision-making (Bamford & Bamford, 2019). Particularly, the striatum receives heavy innervation from the cortex which includes excitatory inputs from both ET and IT neuron populations. Corticostriatal projection terminals, identified as vesicular glutamate transporter-1 (vGluT1) positive, form asymmetric synapses on dendritic spines in the putamen (Fig. 2).

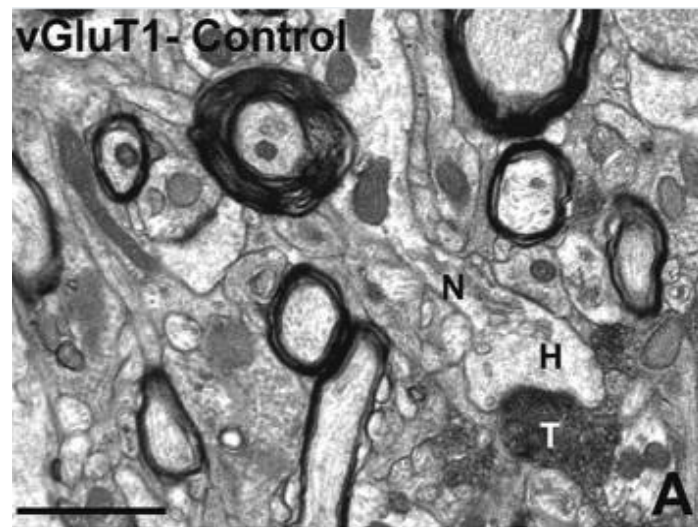


Figure 2. Electron micrograph of a vGluT1 positive corticostriatal terminal (T) in the commissural putamen. The terminal forms an asymmetric synapse with a large postsynaptic density on the head (H) of a dendritic spine. Other abbreviations: N, spine neck. Adapted from “Differential Structural Plasticity of Corticostriatal and Thalamostriatal Axo-Spinous Synapses in MPTP-Treated Parkinsonian Monkeys,” by Villalba & Smith, 2011, *The Journal of Comparative Neurology*, 519(5), p. 989–1005. Copyright 2010 by Wiley-Liss, Inc.

The corticostriatal synapses form a large postsynaptic density which indicates the glutaminergic nature of the terminal (DeFelipe et al., 1988). Furthermore, the corticostriatal terminals had a cross-sectional diameter between 0.5 and 1 μm , extensive postsynaptic density, and formed synapses with large volume spines suggesting that cortical neurons are a main excitatory input to the striatum (Villalba & Smith, 2011). In addition, another striatal study found that cortical neurons made up more than double the number of glutamatergic boutons than thalamic neurons, further indicating the prevalence of cortical inputs in the striatum (Raju et al., 2008).

Currently, there is limited understanding of the extent of axon collateralization of NHP corticostriatal projections, whether they innervate single targets, like the striatum, or project to multiple brain regions (Parent & Parent, 2006; Coudé et al., 2018; Paré & Smith, 1996; Kita & Kita, 2012). One NHP study, using single-cell tracing of corticostriatal neurons, found that these cells do not solely innervate the striatum, but would also project to the brainstem and spinal cord (Parent & Parent, 2006). Similarly, corticosubthalamic neurons also projected to brainstem areas, but not the striatum (Coudé et al., 2018). In agreement with the results in rodents from Kita and Kita (2012), a third study found that corticostriatal neurons would project to the thalamus, specifically the pulvinar nuclei, in cats (Paré & Smith, 1996). As mentioned before, projections from corticospinal neurons in NHPs were found to have high terminal density in the pontine nuclei and the thalamus with other regions, like the red nuclei and pedunculo-pontine tegmental nuclei, also containing corticospinal terminals (Sinopoulou, et al. 2022, Fig. 1). The brain areas in which corticostriatal neurons project and innervate are rudimentary and not well understood in current literature. Given the context of previous literature, we attempt to examine corticostriatal projections in NHPs by utilizing two rhesus monkeys with injections of retrograde adeno-associated viruses (AAV-retro) in the putamen.

Study Goals

The goal of this project is to further characterize the extent of axon collateralization of sensorimotor corticostriatal neurons in NHP. Using AAV-retro injections in the putamen, we determined the ultrastructural features and pattern of synaptic connectivity of the corticostriatal projections in the pontine and pulvinar nuclei of rhesus monkeys. Utilizing immunostaining and electron microscopy, the labeled axon terminals in the pontine nuclei and thalamus will first be characterized morphologically and then compared to corticopontine and corticothalamic terminals labeled in a third monkey injected with an anterograde AAV in the M1. Double immunohistochemistry will further confirm that those axon terminals are collaterals of neurons projecting from the cerebral cortex using vGluT1, a marker of cortical terminals in monkeys. A second double immunostaining with vGluT2 will further confirm that labeled terminals are not from other brain regions that project glutamatergic innervation, such as the striatum and brain stem.

Another objective of this study will be to compare the morphology and synaptic connections seen in the pontine and pulvinar nuclei that receive collaterals from corticostriatal axons with the known ultrastructure of corticostriatal terminals described in previous monkey studies. Through these experiments, we will be able to determine if axon terminals in the pontine nuclei and thalamus that originate from axons of ET corticostriatal neurons display ultrastructural features and patterns of synaptic connection similar to those of corticostriatal terminals. If these findings demonstrate that ultrastructurally different populations of terminals are found in the pontine nuclei, thalamus, and striatum, it will imply that the morphology of terminals that originate from single ET corticostriatal axons in the pontine nuclei and pulvinar is regulated by developmental events or other cues intrinsic to the target nuclei. The results of this

study will lead to a stronger comprehension of corticostriatal projections in NHPs and to improve understanding of motor connectome differences between species, a key piece missing in neuroanatomical work.

Materials and Methods

Viral Vector-Mediated Labeling of Cortical Neurons

Many previous studies have utilized single-cell tracing to identify cortical projections (Parent & Parent, 2006; Coudé et al., 2018; Kita & Kita, 2012). Advantages of this method include precise localization of collaterals and confirmation of cortical origins. However, a shortcoming is the fine detail and time required to amass a large number of samples. Recent findings have demonstrated that an engineered variant of recombinant adeno-associated virus serotype 2 (AAV2-retro) is a highly powerful tool to retrogradely transduce the full dendritic and axonal arbors of corticofugal neurons in primates (Tervo et al., 2016). This method allows for detailed quantitative and morphometric analyses of specific subtypes of neurons identified by their projection targets (Albaugh et al., 2021; Sinopoulou et al., 2022; Weiss et al., 2020). Taking advantage of the unique properties of AAV2-retro, we labeled the extent of axon collateralization of ET corticostriatal neurons that project to the post-commissural sensorimotor putamen in rhesus monkeys.

Animals

Three rhesus monkeys (*Macaca mulatta*) were chosen from the Emory National Primate Research Center breeding colony. All conditions and procedures followed guidelines from the National Institutes of Health and were approved by Emory's Institutional Animal Care and Use Committee. Details of the animals and injections performed are provided in Table 1, The injection surgeries were conducted as previously described (Masilamoni et al., 2024). The monkeys were injected with the respective viral vector (2 μ L) in the respective location 6-8 weeks prior to deep anesthesia with intravenous injection of pentobarbital (100 mg/kg) and

perfusion with a mixture of paraformaldehyde (4%) and glutaraldehyde (0.1%). The brains were immediately removed and post-fixed in paraformaldehyde (4%) for 24 hours before being cut into 60 μ m-thick sections with a vibrating microtome. Serial sections were processed immunohistochemically to localize fluorescent markers using specific primary antibodies, that were revealed with the immunoperoxidase approach.

Monkey ID	Gender	Age	Injection Side	Injection Location	Virus
MR358	Male	4 years old	Left	M1	AAV5-hSyn-GFP
MR363	Female	4 years old	Right	Post-commissural putamen	AAVrg-hSyn-EGFP
MR371	Female	4 years old	Right	Post-commissural putamen	AAVrg-hSyn-mCherry

Table 1. Information of monkeys used in the study, including location and type of viral vector. Both light and electron microscopy were utilized to analyze the tissue from these monkeys.

Immunohistochemistry

Primary antibodies used for immunostaining, including dilutions and vendors, were recorded (Table 2).

Antibody, Catalog #	Dilution	Vendor
GFP - A11122	1:5000	Life Tech
mCherry - 632543	1:2500	Takara
vGluT1 - AB5905	1:5000	Millipore
vGluT2 - VGT2-6	1:1000	MAB Tech

Table 2. Information of antibodies used in the study, including dilutions and vendors.

Light Microscopy

In order to observe the extent of labeling of the putamen/M1 injection, about every 10 sections underwent immunostaining for light microscopy view. The best preserved sections were

selected and placed in sodium borohydride (1%) for 20 minutes. After several rinses in phosphate buffered saline (PBS; 0.1 M, pH 7.4), the sections were incubated for 60 minutes at room temperature in a pre-incubation solution containing 1% normal animal serum, 1% bovine serum albumin (BSA), 0.3% triton, and PBS. Sections were then placed in a primary antibody solution containing the respective primary antibody at its correct dilution, 1% normal animal serum, 1% BSA, 0.3% triton, and PBS for 24 hours at room temperature. The next day, the sections were rinsed and put in a secondary antibody solution consisting of a biotinylated antibody at the correct dilution, 1% normal animal serum, 1% BSA, 0.3% triton, and PBS for 90 minutes at room temperature. After rinsing in PBS, the sections were put in an Avidin-Biotinylated-Complex (ABC) solution with 0.3% triton for 90 minutes at room temperature. After rinses in PBS and a final rinse in tris(hydroxymethyl)aminomethane (TRIS; 0.05M, pH 7.6), immunostaining was revealed using a diaminobenzidine (DAB) solution. This solution contained 48.5 mL of TRIS buffer, 0.5 mL of imidazole (1.0M), 0.0125 g of DAB, and 1 mL hydrogen peroxide (0.3%) and the sections were left in it for 10 minutes at room temperature. Six final rinses were performed to clean the sections of the DAB solution. For storage and visualization, sections were mounted and cover slipped on slides.

Electron Microscopy

To visualize morphology and ultrastructure of sections, a similar protocol to the immunostaining process for light microscopy sections was performed on sections for transmission electron microscopy. Three key differences should be noted between the two immunostaining processes: (1) before pre-incubation, a cryoprotectant protocol of leaving sections in 100% cryoprotectant for 20 minutes at room temperature, then leaving sections outside of solution in a -80°C freezer for 20 minutes, and finally adding sections back in a

sequence of 10 minute serial dilutions of cryoprotectant at room temperature from 100% to PBS (100% → 70% → 50% → 30% → PBS); (2) omitting 0.3% triton from all solutions; and (3) post-DAB processing. The post-DAB processing consists of a series of chemically drying sections. First, a 1% osmium with phosphate buffer (PB) is carefully added to the sections that were placed in PB prior and then placed on a dry watch glass in preparation for the osmium. After 20 minutes at room temperature, the osmium is discarded and PB is used to rinse. The sections are then placed in a 50% alcohol solution for 15 minutes. The following sequence of rinses occur after: 1% uranyl acetate with 70% alcohol for 35 minutes, 90% alcohol for 15 minutes, 100% alcohol for 10 minutes (twice), and propylene oxide for 10 minutes (twice).

The brittle sections are embedded in a resin mixture (Durcupan, Fluka) and baked at 60°C for 48 hours. After the baking period, a tiny piece of the section is removed from the region of interest which is then cut on the ultramicrotome into 60 nm sections that are placed in grids. The grids are stained with lead citrate to improve contrast.

Immunogold for Electron Microscopy

For double immunostaining with gold particles, the same sodium borohydride rinse and cryoprotectant protocol was followed, just like in the electron microscopy procedure. However, the pre-incubation solution of 5% milk and PBS solution for 30 minutes at room temperature was used. Rinses were then done in TBS-Gelatin. The primary solution was 1% milk, the primary antibody dilution, and TBS-Gelatin which the sections were left overnight at room temperature. The secondary solution contained 1% milk, the secondary antibody dilution, and TBS-gelatin where the sections were left in it for 2 hours at room temperature. After the secondary antibody solution, the sections were washed in a 2% aqueous Acetate buffer (~7.0 pH). A HQ kit was used in a dark room until immunostaining appeared. Subsequent rinses in aqueous acetate then

TBS-Gelatin were performed and a 90 minute incubation was done in an ABC solution with 1% milk and TBS-Gelatin at room temperature. After the ABC incubation and rinses in TBS-Gelatin (twice) and Tris (once), DAB protocols were followed which was then proceeded by the dehydration and embedding steps.

Image Analysis

Light Microscopy

The light microscopy prepared sections were scanned with Aperio ScanScope CS system (Aperio Technologies, Vista, CA) and viewed using ImageScope software (Aperio Technologies). Specifically, any areas, especially subcortical regions, were scanned for terminals with labeling. Those areas were noted and a high magnification picture was taken.

Electron Microscopy

Grids were taken from areas with heavy terminal labeling in the light microscopy prepared counterpart. The electron microscopy prepared grids were examined under a JEOL JEM 1011 transmission electron microscope and images were taken using an Erlagshen ES1000W Gatan Camera. Images of terminals with heavy peroxidase deposits and forming a synapse were taken at 40,000x magnification. For immunogold, a criterion of at least 3 gold particles was used to count a terminal as immunogold positive. In addition to the immunogold positive aspect and the aforementioned requirements, 40,000x magnification images were also taken of terminals that were characterized by those parameters.

Statistical Analysis

The study is currently incomplete due to lack of sample size of subjects and number of terminal data points. As a result, statistical analysis was purposefully not performed on the data as results may be inconsistent with small/non-existent sample sizes. However once the project reaches completion, one-way ANOVA will be used to test for statistical significance between the different sizes of terminals as well as between postsynaptic target sizes in the pontine and pulvinar nuclei.

Results

Localization of Viral Vector Labeling by Light Microscopy

After injection of the AAV-retro in the putamen of monkey MR363 and LM immunohistochemical processing using a GFP antibody, a clear snapshot of labeling in different slices of the brain could be seen (Fig. 3). More specifically, there was intense labeling of pyramidal neurons in the motor area 6 cortex (6M), M1, and primary somatosensory cortex (S1), among other cortical regions. The post-commissural putamen of this monkey was highly labeled as well, indicating diffusion of the viral vector after the injection. There was no spread of the injection site beyond the confines of the putamen.

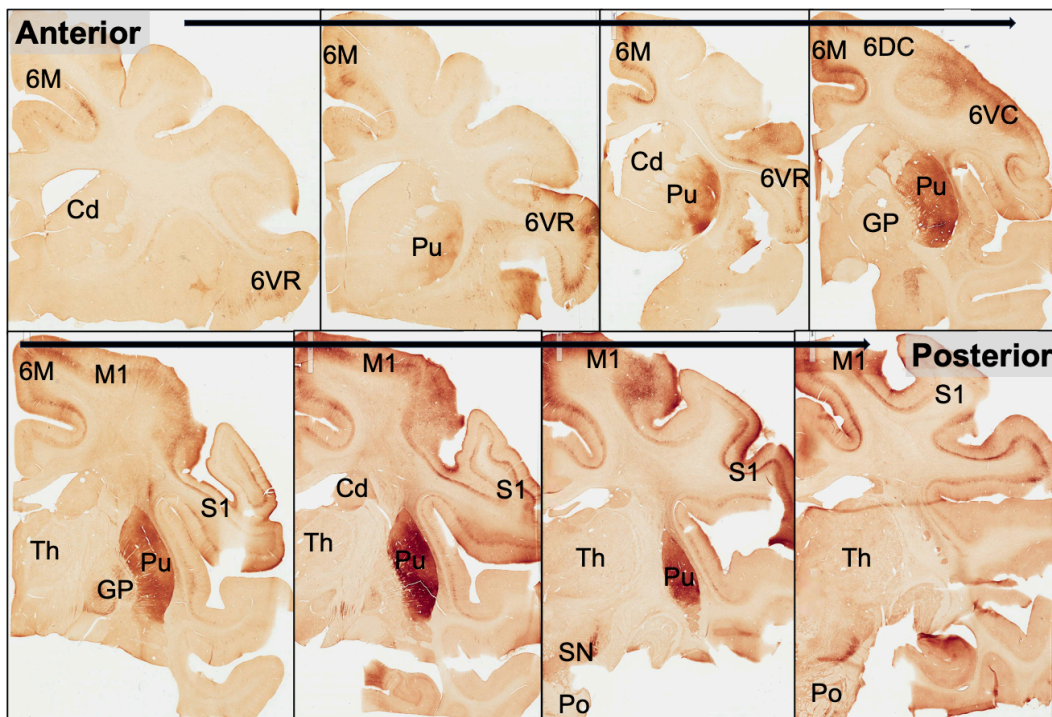


Figure 3. Low-power light microscopy images from coronal slices at different antero-posterior levels of MR363R showing GFP-positive retrogradely labeled layer 5 pyramidal neurons after injections of AAV2-Retro in the postcommissural putamen. Note the extensive retrograde labeling in motor and somatosensory cortices. Abbreviations: 6M, motor area 6; Cd, caudate nuclei; 6VR and 6VC, ventral premotor area; Pu, putamen; 6DC, dorsal premotor area; GP, globus pallidus; Th, thalamus; S1, primary somatosensory area; SN, substantia nigra; Po, pontine nuclei.

Following analysis of serial sections through the monkey brain, two brain regions were found to contain a significant amount of labeled axonal and terminal profiles. Under closer examination, both the pontine and pulvinar nuclei of the thalamus contained clusters of GFP-labeled terminals (Fig. 4). The pontine nuclei (Fig. 4B, 4C) are more densely labeled than the pulvinar nuclei (Fig. 4D, 4E) which suggests greater innervation of the pontine nuclei from retrogradely labeled neurons.

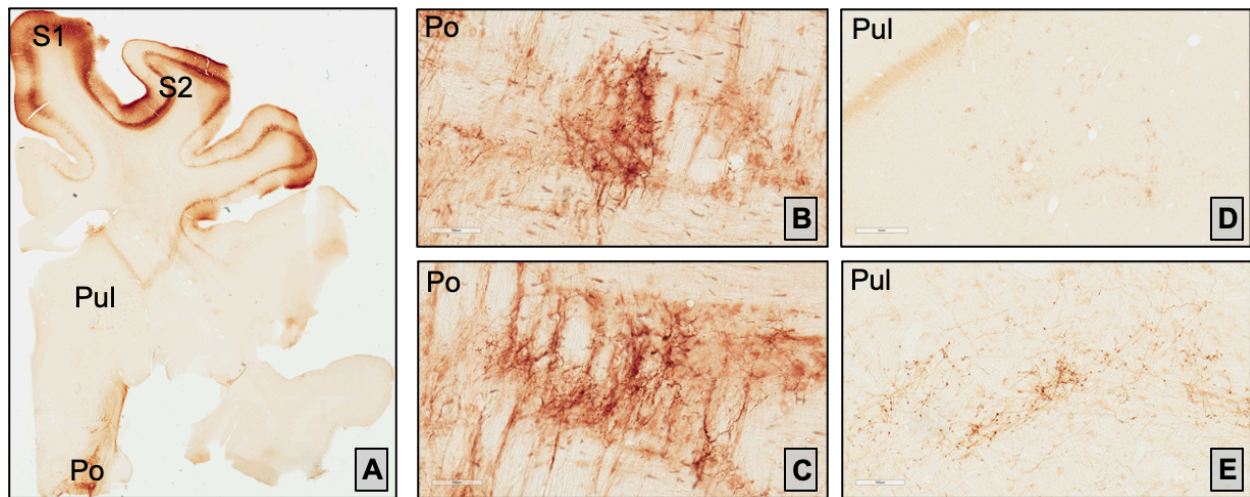


Figure 4. Low- and high-power light microscopy images of GFP-positive terminal labeling in the pontine nuclei (A,B,C) and pulvinar (A,D,E) after AAV2-retro injection in the putamen of monkey MR363R. Note heavy retrograde transduction of pyramidal neurons in M1 and S1 cortices. Abbreviations: S1, primary somatosensory area; S2, secondary somatosensory area; Pul, pulvinar nuclei; Po, pontine nuclei.

To determine if the retrogradely labeled neurons in M1 potentially contributed to the pulvinar and pontine nuclei innervation seen after AAV2-retro injection in the putamen, we analyzed the pattern of terminal labeling in these nuclei after injection of an anterograde AAV in the arm region of M1 in monkey MR358. All layers of the arm region of M1 were densely labeled and the viral vector diffused into the underlying white matter (Fig. 5A). This injection resulted in strong anterograde labeling of the post-commissural putamen, which is consistent with the expected innervation from the retrogradely labeled M1 neurons in monkey MR363 (Fig. 5A). Relative to the AAV-retro injection in the putamen, the pontine nuclei also contained large

amounts of labeled axons and terminals following M1 injections (Fig. 5B, 5C). On the other hand, although the pulvinar nuclei contained rich plexuses of labeled terminals after M1 injections, the morphology of these terminals was different from the labeling found after AAV2-retro injection in the putamen. Instead of being large and confined to small clusters distributed throughout the nucleus as depicted in figure 4D-E, the pulvinar labeling after M1 injection was more diffuse and made up of small-sized terminal profiles (Fig. 5D-E). The results of these experiments suggest that the innervation of the pontine nuclei after AAV2-retro injection in the putamen may originate in part from M1, while that of the pulvinar likely arises from another cortical region.

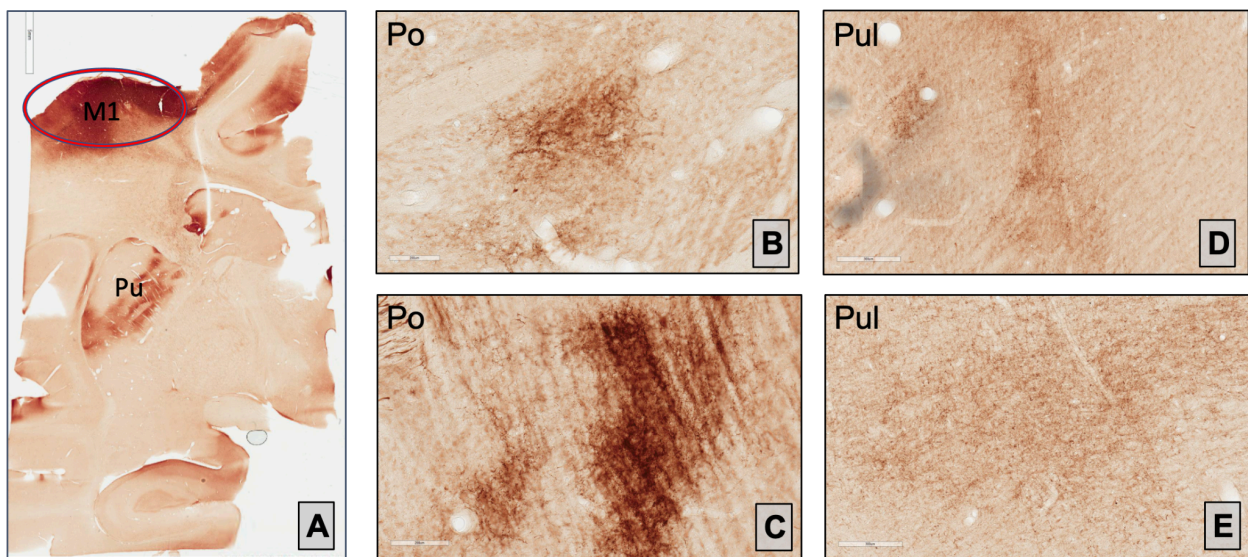


Figure 5. Low- and high-power light microscopy images of GFP-positive terminal labeling in the pontine nuclei (B,C) and pulvinar (D,E) after anterograde AAV5 injection in the M1 of monkey MR358L. Note heavy anterograde labeling in putamen. Abbreviations: M1, primary motor area; Pu, putamen; Po, pontine nuclei; Pul; pulvinar nuclei.

Ultrastructure Characterization of Corticopontine and Corticothalamic Projections – Electron Microscopy

To further assess the possible cortical origin of labeled terminals in the pontine nuclei and pulvinar after AAV-retro injections in the putamen, we used electron microscopy and vGluT1 immunohistochemistry to study the ultrastructure, the pattern of synaptic connections and the transmitter content of these terminals. After EM processing, sections of clustered, labeled terminals from both the pontine nuclei and the pulvinar nuclei were extracted and examined under a transmission electron microscope. From the images taken, a total of 328 GFP- or mCherry-labeled terminals forming clear synapses in the pontine nuclei were analysed from monkeys MR363 and MR371. Labeled terminals varied in size from smaller than 0.5 μm to larger than 3.0 μm in cross-sectional diameter with most terminals being between 1.0 to 3.0 μm . All terminals also contained multiple mitochondria. Of the 328 terminals, 327 formed asymmetric axo-dendritic synapses and 1 formed an asymmetric axo-axonic synapse in a triad formation with one unlabeled terminal and one dendrite (Fig 6A, 6B, 7A). The axo-axonic synapse was extremely rare as all other synapses were axo-dendritic. Postsynaptic dendrite sizes were variable ranging from small- (<0.5 μm in cross-sectional diameter), medium- (0.5 μm – 1 μm in cross-sectional diameter), large- (1.0 μm – 3.0 μm in cross-sectional diameter), and extra large- (>3.0 μm in cross-sectional diameter) (Fig. 9). GFP-labeled terminals often terminated on a single postsynaptic target (Fig. 6A), but a third of terminals formed multi-synapses (Fig. 6B).

After double immuno-EM experiments were completed using immunoperoxidase staining for GFP combined with pre-embedding immunogold labeling for vGluT1 or vGluT2, an identical procedure of selecting sections as the single immuno-EM experiment was performed. Terminals were considered vGluT1 or vGluT2 positive if three or more immunogold particles were present

in the terminal. vGluT1+/GFP+ terminals followed a similar morphological and termination pattern as the labeled terminals from the single immuno-EM experiment (Fig. 6C, 6D). All vGluT1+/GFP+ terminals formed axo-dendritic synapses, except in one case where an axo-axonic synapse was observed (Fig. 6C, 6D, 7B). Of the 49 GFP+ terminals examined, all were also vGluT1-positive indicating their cortical origin. On the other hand, none of the 6 GFP+ terminals examined in vGluT2-immunostained tissue were double labeled for vGluT2+, further supporting the evidence that vGluT1+ corticostriatal neurons are the main source of these corticopontine terminals (Fig. 6E, 6F). Neurons positive for vGluT2 can often be found from neurons that originate from the thalamus, striatum, and brain stem. As a result, it is likely that the few vGluT2+ terminals observed were due to a small extent of anterograde transport from the putamen injection, a limitation of the AAV-retro.

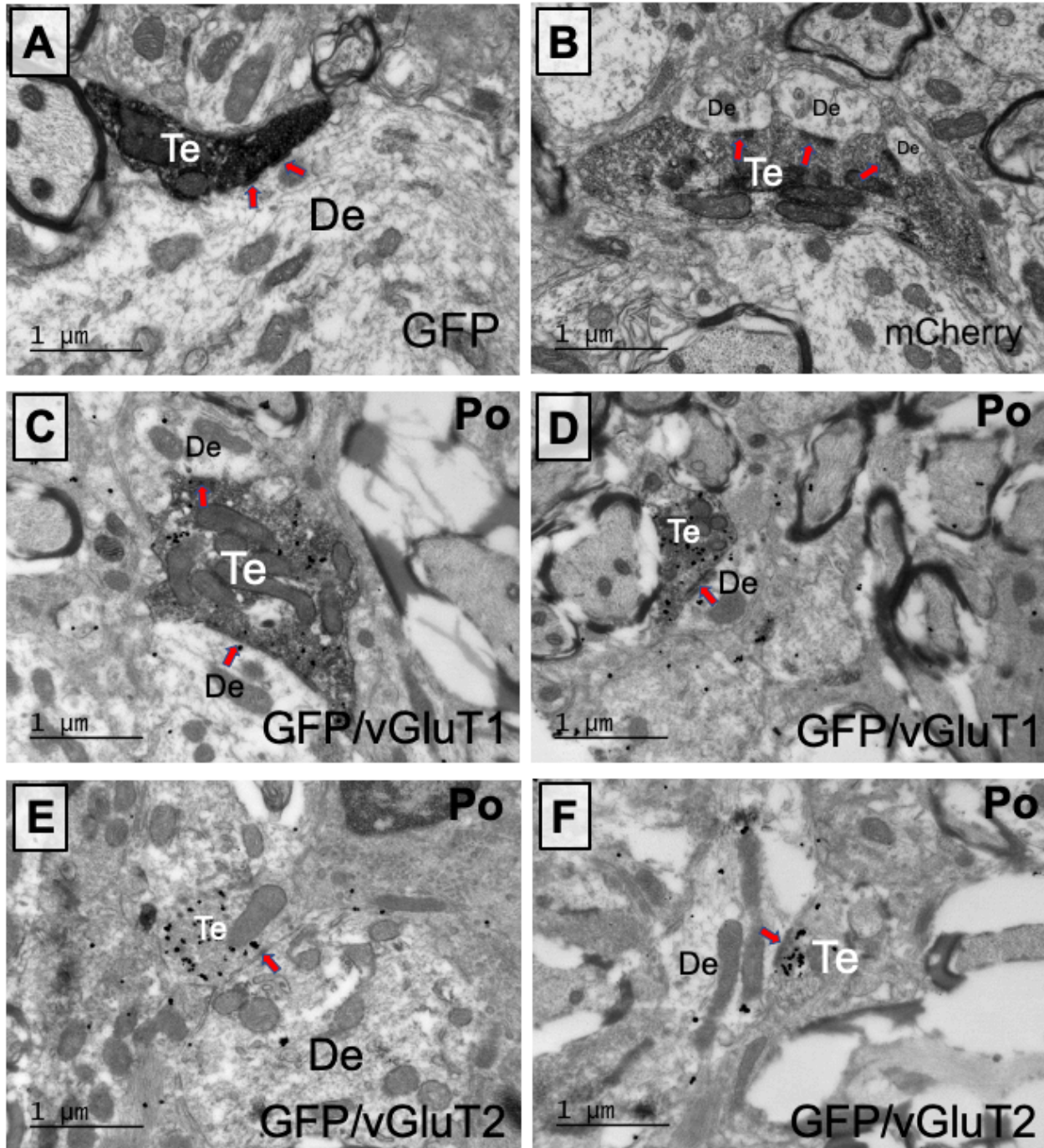


Figure 6. Electron micrographs of labeled axon terminals forming asymmetric synapses in the pontine nuclei after injections of AAV2-retro in the putamen from MR363R and MR371R. In the pontine nuclei, most labeled terminals form synapses with dendrites of various sizes. (A,B) GFP+ or mCherry+ terminals. (C,D) GFP+ terminals that co-express vGluT1 confirming their cortical origin. (E,F) vGluT2+/GFP- terminals in the pontine nuclei after AAV2-retro injections in the putamen. None of the GFP+ terminals in the pontine nuclei labeled after AAV2-retro injections in the putamen expressed vGluT2 immunoreactivity. Red arrows indicate synapses. Scale bars are in the lower left corner of each image. Abbreviations: Te, terminal; De, dendrite.

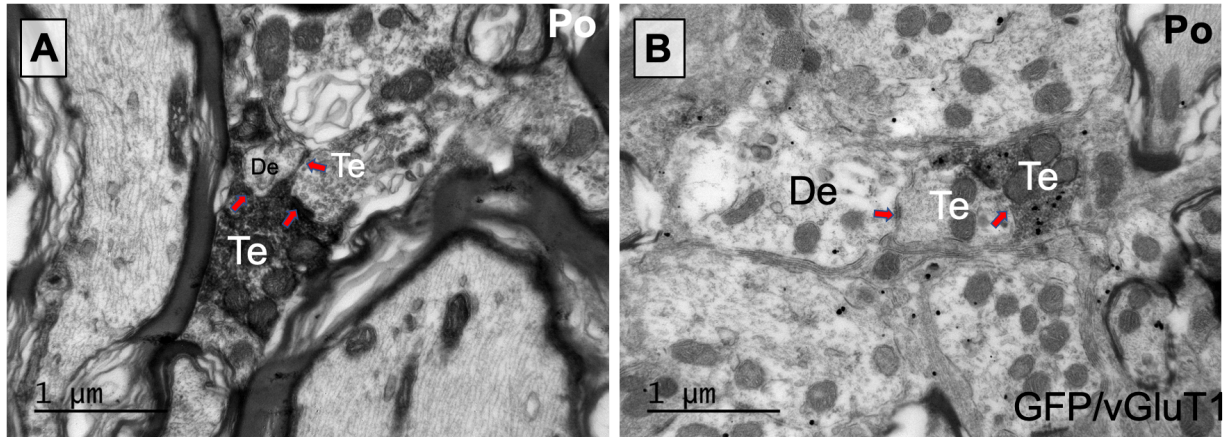


Figure 7. Electron micrographs of labeled axon terminals forming asymmetric axo-axonic synapses in the pontine nuclei after injections of AAV2-retro in the putamen from MR363R and MR371R. **(A)** In the pontine nuclei, there is a triad formation with a GFP labeled terminal, an unlabeled terminal, and a dendrite. **(B)** In double immunostaining, there is another axo-axonic synapse. Red arrows indicate synapses. Scale bars are in the lower left corner of each image. Abbreviations: Te, terminal; De, dendrite.

In comparison to the AAV-retro-labeled terminals in the pontine nuclei, terminals found in the pulvinar of the same monkeys are similar in morphology in terms of cross-sectional diameter, multi-synapses, and number of mitochondria (Fig. 8). However, between the two brain regions, the terminals targeted distinct postsynaptic targets. In the pontine nuclei, all but one postsynaptic target were dendrites. Contrarily, in the pulvinar nuclei, more than half of postsynaptic targets were on vesicle-filled elements (Fig. 10). Between the two nuclei, the relative distribution of sizes of postsynaptic targets tended to be similar with slightly larger (maybe more proximal) postsynaptic targets in the pulvinar nuclei (Fig. 9). When comparing diameters of the postsynaptic targets in the pulvinar nuclei, postsynaptic element sizes were similar, with the dendritic targets being slightly more proximal than the vesicle-filled elements (Fig. 10).

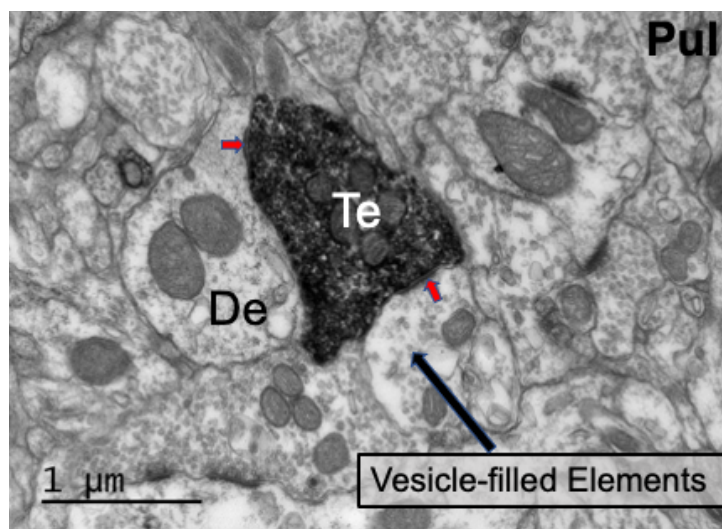


Figure 8. Electron micrograph of GFP-labeled axon terminals forming asymmetric synapses in the pulvinar nuclei after injections of AAV2-retro in the putamen from MR371R. In the pulvinar nuclei, there is a slight majority of GFP-labeled terminals forming synapses on vesicle-filled elements rather than axo-dendritic synapses. However, many single terminals form synapses with a combination of the two types of postsynaptic targets. Red arrows indicate synapses. Scale bars are in the lower left corner of the image. Abbreviations: Te, terminal; De, dendrite.

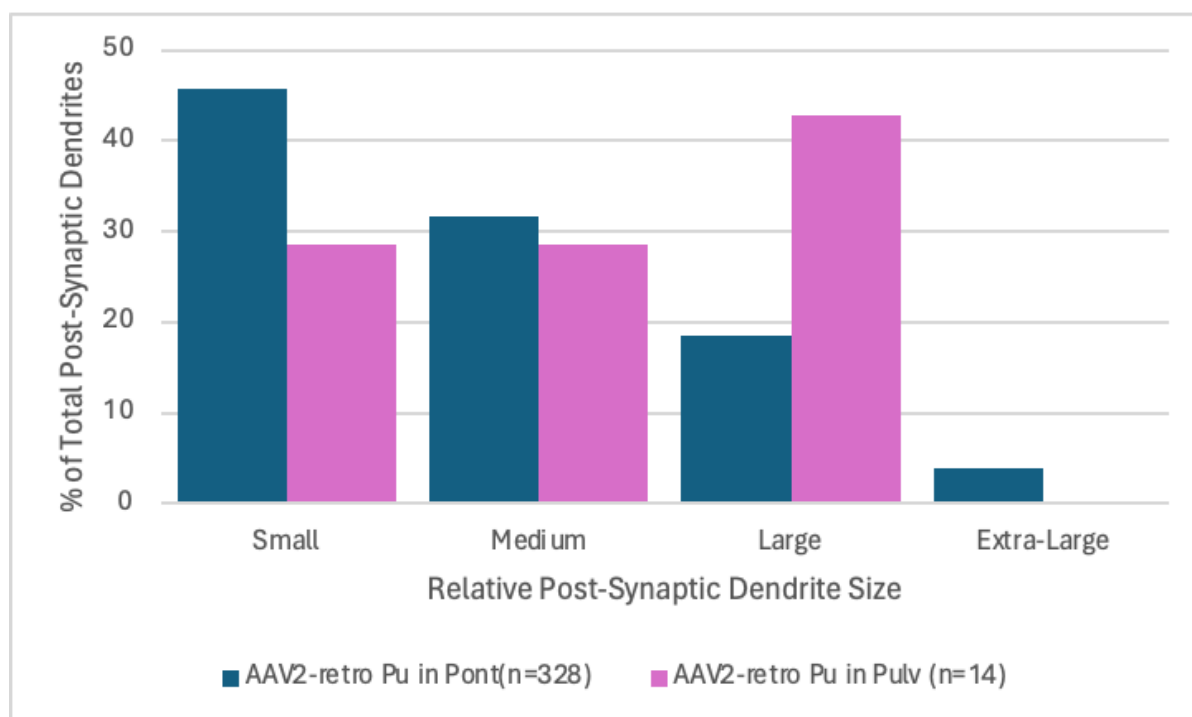


Figure 9. Histogram showing the proportion of dendrites of various sizes innervated by labeled axon terminals in the pontine nuclei (navy bars) and the pulvinar (pink bars). Dendrites were categorized in the following groups based on their cross-sectional diameter: Small $\leq 0.5 \mu\text{m}$. Medium = $0.5 - 1.0 \mu\text{m}$. Large = $1.0 - 3.0 \mu\text{m}$. Extra Large $\geq 3.0 \mu\text{m}$. Data on terminals forming axo-axonic synapses are not included.

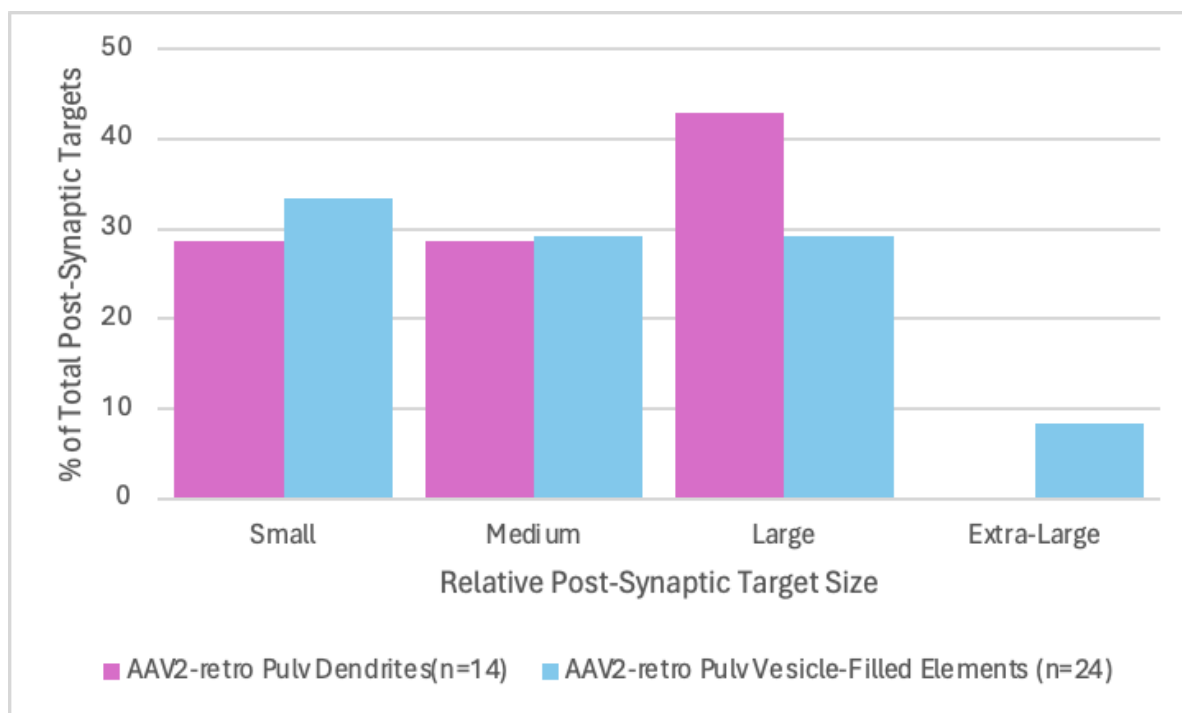


Figure 10. Histogram showing the proportion of elements of various sizes innervated by labeled axon terminals in the pulvinar nuclei. Pink bars represent dendrites and light blue bars represent vesicle-filled elements. Dendrites were categorized in the following groups based on their cross-sectional diameter: Small $\leq 0.5 \mu\text{m}$. Medium = $0.5 - 1.0 \mu\text{m}$. Large = $1.0 - 3.0 \mu\text{m}$. Extra Large $\geq 3.0 \mu\text{m}$.

Ultrastructure Characterization of Corticopontine Terminals labeled by M1 Anterograde AAV Injection vs Putamen Retrograde AAV Injection

In the pontine nuclei, labeled terminals after injections of AAV5 in M1 or AAV-Retro in putamen were morphologically similar (Fig. 11). The general trend for postsynaptic targets in the pontine nuclei was a majority of small-diameter (most likely distal) dendrites, but a significant number of terminals also contacted medium-sized and large-sized dendrites suggesting that these terminals target the whole proximo-distal extent of the dendritic tree of neurons in the pontine nuclei (Fig. 12). Because we have not analyzed the morphology and pattern of synaptic connection of terminals labeled in the pulvinar nuclei after M1 injections, a similar comparative analysis could not be done for corticothalamic terminals.

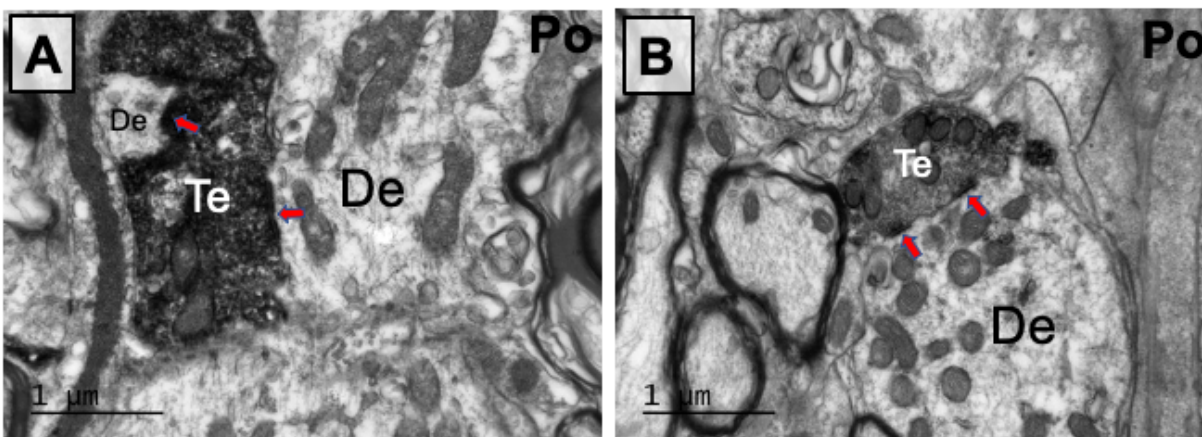


Figure 11. Electron micrograph of GFP-labeled axon terminals forming asymmetric synapses in the pontine nuclei after injections of anterograde AAV5 in the M1 of MR358L. Synaptic patterns and morphological characterization mirrored very similarly to terminals found in the pontine nuclei of the AAV2-retro injected monkey. Red arrows indicate synapses. Scale bars are in the lower left corner of each image. Abbreviations: Te, terminal; De, dendrite.

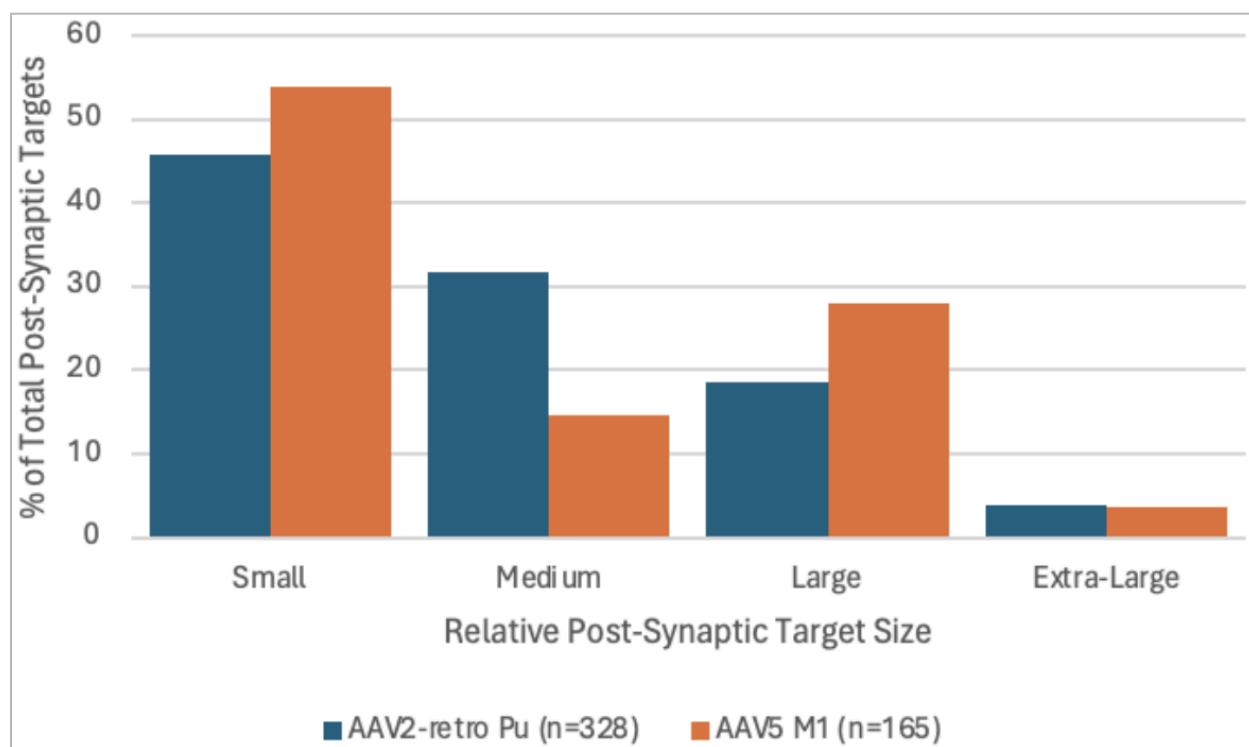


Figure 12. Histogram showing the proportion of dendrites of various sizes in the pontine nuclei innervated by labeled axon terminals. Dendrites were categorized in the following groups based on their cross-sectional diameter: Small $\leq 0.5 \mu\text{m}$. Medium = $0.5 - 1.0 \mu\text{m}$. Large = $1.0 - 3.0 \mu\text{m}$. Extra Large $\geq 3.0 \mu\text{m}$.

Discussion

Collaterals of Corticostriatal Axonal Projections Throughout the Brain

Based on data collected from AAV-retro injections in the putamen of rhesus monkeys, we suggest that the main targets of axon collaterals of ET corticostriatal neurons are the pontine and pulvinar nuclei. IT neuron populations were able to be ruled out as part of the ET corticostriatal neurons targeting these areas since the pontine and pulvinar nuclei reside outside of the telencephalon. Excluding these two brain regions, light microscopy analysis of serial sections through the whole rostro-caudal extent of the brain of these monkeys indicate that other brain regions are almost completely devoid of collateral innervation from ET corticostriatal neurons (Fig. 3).

In terms of the pontine nuclei, labeled terminals after injections of AAV-Retro in the putamen or AAV5 in M1 were morphologically similar. They formed dense clusters of large-sized terminals throughout the pontine nuclei (Fig. 4B, 4C, 5B, 5C). However, when comparing the AAV-retro injection in the putamen and the anterograde AAV injection in the M1, there were differences in the innervation pattern of the pulvinar nuclei. The corticothalamic terminals labeled after injections of AAV-retro in the putamen depicted a scarce, cluster-like innervation pattern (Fig. 4D, 4E), whereas terminals labeled after M1 injections of AAV5 were smaller in size and much more evenly dispersed throughout the nucleus (Fig. 5D, 5E).

Rodent studies have indicated a larger innervation of thalamic regions by layer 6 neurons from the M1 compared to layer 5a/5b neurons of the M1 (Hoerder-Suabedissen et al., 2018). The authors noted that layer 6 projections to the posterior thalamic nuclei had a more widespread pattern of innervation whereas layer 5 projections were clustered in those same regions. Given this literature, it is possible that the diffuse terminal labeling seen in the pulvinar after M1

injection of AAV5 originates from layer 6 neurons of M1, whereas the clusters of large terminals seen after injections of AAV-retro in the putamen originates from collaterals of layer 5 corticostriatal neurons located in another cortical region. A possible cortical region could be the somatosensory cortex as another study previously reported this connection to exist (Paré & Smith, 1996). However, given the lack of electron microscopic data on the labeled M1 corticothalamic terminals, any assertions on the morphology of the observed innervation cannot be made.

Immunoreactivity for vGluT1 in Corticostriatal Projection Terminals in Pontine Nuclei and Verification of Morphology in Comparison to Corticopontine and Corticothalamic Neurons

Our findings indicate complete colocalization of vGluT-1 gold particles with GFP labeled terminals in the AAV-retro injected monkey (MR363). Given vGluT1's role in glutamate transport in cortical neurons, these results confirm the cortical origins of those terminals which further supports the effectiveness of the AAV-retro viral vector in labeling axon collaterals of corticostriatal neurons. Furthermore, vGlut2 was not found to be colocalized with any GFP labeled terminals in the same monkey. vGlut2 is a glutamate transporter found in neurons from other brain areas, so we can rule out any of the labeled terminals as being non-cortical.

The ultrastructure of cortico-pontine terminals labeled after AAV-Retro in the putamen was also in-line with the morphology of terminals found in the pontine nuclei after anterograde AAV injection in M1. In both cases, terminals were large, filled with mitochondria, and formed multiple asymmetric axo-dendritic synapses. Overall, these observations suggest that axon collaterals of M1 corticostriatal neurons innervate the pontine nuclei. However, such may not be the case in the pulvinar based on the different pattern of regional innervation (diffuse vs clustered) and size (small vs large) of the labeled terminal profiles seen after striatal AAV-retro

or M1 AAV5 injections. Additional electron microscopic analysis of M1 labeled terminals in the pulvinar is needed to compare their ultrastructure and synaptic connections with terminals labeled after striatal injections of AAV-Retro.

Differences in Morphology of Postsynaptic Targets Between Collaterals of Corticostriatal Projections in Pontine and Pulvinar Nuclei

As expected, collaterals of corticostriatal projections to the pontine and pulvinar nuclei give rise to terminals that formed asymmetric synapses with postsynaptic targets. Terminals were very similar in cross-sectional diameter and mitochondria count. However, the type of postsynaptic targets differed although proximity of those targets in each brain region remained similar between the two sets of projections.

In the pontine nuclei, the overwhelming majority (>99.5%) of postsynaptic targets were dendrites of varying sizes from smaller than 0.5 μm to some over 3.0 μm in cross-sectional diameter. Over 76% of dendrites were smaller than 1.0 μm which indicates how distal the synapses were from the cell body of the postsynaptic neuron. In the pulvinar, a slight majority (63%) of postsynaptic targets were to a vesicle-filled element and the other targets were also dendrites of varying sizes. When comparing the sizes of postsynaptic targets between those found in the pontine nuclei and those found in the pulvinar nuclei, in both structures the dendrites targeted were, in general, less than 1.0 μm in diameter (Fig. 9).

The vesicle-filled elements could possibly be dendrites or terminals of GABAergic interneurons. In a study with cats, similar results were found, i.e. collaterals of corticostriatal projections to the thalamus were found to innervate on, what the authors believed to be, vesicle-filled dendrites (Paré & Smith, 1996). However, given this information, it may be difficult to classify the vesicle-filled elements as dendrites. Neuron terminals are filled with

vesicles of neurotransmitters, but another notable feature of these terminals are the synapses they form. However, these elements could still be terminals that are not forming synapses at the particular level the image was taken. One thing to note is that there were zero instances where the vesicle-filled elements did end up forming a synapse in a terminal-like fashion, but it is important to take precaution from making assumptions on the type of element without further verification.

Comparison of Morphology Between Corticostriatal, Corticopontine, and Corticothalamic Terminals

Based on studies from the literature (Villalba & Smith, 2011), corticostriatal terminals are strikingly different in morphology and synaptic connection from the corticopontine and corticothalamic terminals labeled after AAV-Retro injection in the putamen. Corticostriatal terminals tend to be small ($<1.0 \mu\text{m}$ diameter) in size, form single synapses, and terminate on the head of dendritic spines. Corticopontine terminals are much larger in size ($>1.0 \mu\text{m}$ diameter), form multi-synapses, and terminate on dendrites. Similarly, corticothalamic terminals in the pulvinar are large and form multi-synapses with both dendrites and vesicle-filled neuronal elements.

From the results of this study, we are able to confirm that these varying populations of terminals in different brain regions may all come from the same, single neuron. There is a possibility that there are two subsets of corticostriatal ET populations: ET neurons that project to only the striatum and thalamus and another group of ET neurons that project to only the striatum and pontine nuclei. However, further verification would be required to confirm the exact innervation patterns of these ET neurons. Yet, the possibility that neurons could form extremely distinct innervation patterns on different populations of neurons in varying brain regions could

lead to a novel discovery of the NHP connectome. These results can serve as the basis for future electrophysiological experiments to assess how certain attributes, like synaptic strength and function, differ in a single neuron.

Limitations for Current Study and Future Directions

As noted throughout the results and discussion, the sample size of the pulvinar nuclei data is limited. Larger data collection will ultimately lead to more rigorous analysis of the data found in this study. Furthermore, statistical analysis of the data is unrealistic and could result in errors as there were extremely large differences in the number of the samples for each neuron population. In that vein, there is also a lack of sample size of total monkeys and a limited diversity of the monkeys that were used in this study (Table 1). Both monkeys in the AAV-retro putamen injection were very similar in basic demographic information. An addition of pulvinar data and more monkeys (to diversify the demographic) to the corticostriatal projection experiment could lead to unexpected results that were unaccountable in the current study.

Another obstacle the study faced was the ultimate objective to compare the normal-state to the parkinsonian-state of the monkeys and observing the change in innervation patterns. One of the limitations is that a large proportion of rhesus macaques endogenously have neutralizing antibodies against various AAV serotypes, making it difficult to expand the AAV tracing procedure used in this study to other monkeys. In the future, we plan to use 1-methyl-4-phenyl-1,2,3,6-tetrahydropyridine (MPTP) induced monkeys to compare the projectome pattern to the current study. Many studies have indicated a change in synaptic connection of a variety of different brain regions between control and MPTP-induced monkeys (Vilalba & Smith, 2011; Masilamoni et al., 2024; Albaugh et al., 2021). These results will improve our understanding of corticostriatal projection patterns to the pontine and pulvinar

nuclei in the Parkinsonian state which is imperative for furthering neuroanatomical work on Parkinson's disease.

References

- Albaugh, D. L., Huang, C., Ye, S., Paré, J. F., & Smith, Y. (2021). Glutamatergic inputs to GABAergic interneurons in the motor thalamus of control and parkinsonian monkeys. *The European journal of neuroscience*, 53(7), 2049–2060.
<https://doi.org/10.1111/ejn.14763>
- Bamford, I. J., & Bamford, N. S. (2019). The Striatum's Role in Executing Rational and Irrational Economic Behaviors. *The Neuroscientist : a review journal bringing neurobiology, neurology and psychiatry*, 25(5), 475–490.
<https://doi.org/10.1177/1073858418824256>
- Bortoff, G. A., & Strick, P. L. (1993). Corticospinal terminations in two new-world primates: further evidence that corticomotoneuronal connections provide part of the neural substrate for manual dexterity. *The Journal of neuroscience : the official journal of the Society for Neuroscience*, 13(12), 5105–5118.
<https://doi.org/10.1523/JNEUROSCI.13-12-05105.1993>
- Coudé, D., Parent, A., & Parent, M. (2018). Single-axon tracing of the corticosubthalamic hyperdirect pathway in primates. *Brain structure & function*, 223(9), 3959–3973.
<https://doi.org/10.1007/s00429-018-1726-x>
- DeFelipe, J., Conti, F., Van Eyck, S. L., & Manzoni, T. (1988). Demonstration of glutamate-positive axon terminals forming asymmetric synapses in cat neocortex. *Brain research*, 455(1), 162–165. [https://doi.org/10.1016/0006-8993\(88\)90127-8](https://doi.org/10.1016/0006-8993(88)90127-8)
- Garcia, A. F., Crummy, E. A., Webb, I. G., Nooney, M. N., & Ferguson, S. M. (2021). Distinct populations of cortical pyramidal neurons mediate drug reward and aversion. *Nature communications*, 12(1), 182. <https://doi.org/10.1038/s41467-020-20526-0>

- Hoerder-Suabedissen, A., Hayashi, S., Upton, L., Nolan, Z., Casas-Torremocha, D., Grant, E., Viswanathan, S., Kanold, P. O., Clasca, F., Kim, Y., & Molnár, Z. (2018). Subset of Cortical Layer 6b Neurons Selectively Innervates Higher Order Thalamic Nuclei in Mice. *Cerebral cortex* (New York, N.Y. : 1991), 28(5), 1882–1897. <https://doi.org/10.1093/cercor/bhy036>
- Jankowska, E., Padel, Y., & Tanaka, R. (1975). Projections of pyramidal tract cells to alpha-motoneurons innervating hind-limb muscles in the monkey. *The Journal of physiology*, 249(3), 637–667. <https://doi.org/10.1113/jphysiol.1975.sp011035>
- Jawabri, K. H., & Sharma, S. (2023). *Physiology, Cerebral Cortex Functions*. In StatPearls. StatPearls Publishing.
- Kita, T., & Kita, H. (2012). The subthalamic nucleus is one of multiple innervation sites for long-range corticofugal axons: a single-axon tracing study in the rat. *The Journal of neuroscience : the official journal of the Society for Neuroscience*, 32(17), 5990–5999. <https://doi.org/10.1523/JNEUROSCI.5717-11.2012>
- Masilamoni, G. J., Kelly, H., Swain, A. J., Pare, J. F., Villalba, R. M., & Smith, Y. (2024). Structural Plasticity of GABAergic Pallidothalamic Terminals in MPTP-Treated Parkinsonian Monkeys: A 3D Electron Microscopic Analysis. *eNeuro*, 11(3), ENEURO.0241-23.2024. <https://doi.org/10.1523/ENEURO.0241-23.2024>
- Paré, D., & Smith, Y. (1996). Thalamic collaterals of corticostriatal axons: their termination field and synaptic targets in cats. *The Journal of comparative neurology*, 372(4), 551–567. [https://doi.org/10.1002/\(SICI\)1096-9861\(19960902\)372:4<551::AID-CNE5>3.0.CO;2-3](https://doi.org/10.1002/(SICI)1096-9861(19960902)372:4<551::AID-CNE5>3.0.CO;2-3)

- Parent, M., & Parent, A. (2006). Single-axon tracing study of corticostriatal projections arising from primary motor cortex in primates. *The Journal of comparative neurology*, 496(2), 202–213. <https://doi.org/10.1002/cne.20925>
- Raju, D. V., Ahern, T. H., Shah, D. J., Wright, T. M., Standaert, D. G., Hall, R. A., & Smith, Y. (2008). Differential synaptic plasticity of the corticostriatal and thalamostriatal systems in an MPTP-treated monkey model of parkinsonism. *The European journal of neuroscience*, 27(7), 1647–1658. <https://doi.org/10.1111/j.1460-9568.2008.06136.x>
- Reiner, A., Hart, N. M., Lei, W., & Deng, Y. (2010). Corticostriatal projection neurons - dichotomous types and dichotomous functions. *Frontiers in neuroanatomy*, 4, 142. <https://doi.org/10.3389/fnana.2010.00142>
- Rockland K. S. (2018). Axon Collaterals and Brain States. *Frontiers in systems neuroscience*, 12, 32. <https://doi.org/10.3389/fnsys.2018.00032>
- Saberi, A., Paquola, C., Wagstyl, K., Hettwer, M. D., Bernhardt, B. C., Eickhoff, S. B., & Valk, S. L. (2023). The regional variation of laminar thickness in the human isocortex is related to cortical hierarchy and interregional connectivity. *PLoS biology*, 21(11), e3002365. <https://doi.org/10.1371/journal.pbio.3002365>
- Shepherd G. M. (2013). Corticostriatal connectivity and its role in disease. *Nature reviews. Neuroscience*, 14(4), 278–291. <https://doi.org/10.1038/nrn3469>
- Sinopoulou, E., Rosenzweig, E. S., Conner, J. M., Gibbs, D., Weinholtz, C. A., Weber, J. L., Brock, J. H., Nout-Lomas, Y. S., Ovruchesky, E., Takashima, Y., Biane, J. S., Kumamaru, H., Havton, L. A., Beattie, M. S., Bresnahan, J. C., & Tuszynski, M. H. (2022). Rhesus macaque versus rat divergence in the corticospinal projectome. *Neuron*, 110(18), 2970–2983.e4. <https://doi.org/10.1016/j.neuron.2022.07.002>

- Tervo, D. G., Hwang, B. Y., Viswanathan, S., Gaj, T., Lavzin, M., Ritola, K. D., Lindo, S., Michael, S., Kuleshova, E., Ojala, D., Huang, C. C., Gerfen, C. R., Schiller, J., Dudman, J. T., Hantman, A. W., Looger, L. L., Schaffer, D. V., & Karpova, A. Y. (2016). A Designer AAV Variant Permits Efficient Retrograde Access to Projection Neurons. *Neuron*, 92(2), 372–382. <https://doi.org/10.1016/j.neuron.2016.09.021>
- Villalba, R. M., & Smith, Y. (2011). Differential structural plasticity of corticostriatal and thalamostriatal axo-spinous synapses in MPTP-treated Parkinsonian monkeys. *The Journal of comparative neurology*, 519(5), 989–1005. <https://doi.org/10.1002/cne.22563>
- Weiss, A. R., Liguore, W. A., Domire, J. S., Button, D., & McBride, J. L. (2020). Intra-striatal AAV2.retro administration leads to extensive retrograde transport in the rhesus macaque brain: implications for disease modeling and therapeutic development. *Scientific reports*, 10(1), 6970. <https://doi.org/10.1038/s41598-020-63559-7>